Carbohydrate Polymers 117 (2015) 941–949

Contents lists available at ScienceDirect

Carbohydrate Polymers

journal homepage: www.elsevier.com/locate/carbpol

Electrospun aligned poly(propylene carbonate) microfibers with chitosan nanofibers as tissue engineering scaffolds

Xin Jing[a,b], Hao-Yang Mi[a,b], Jun Peng[b,c], Xiang-Fang Peng[a,*], Lih-Sheng Turng[b,c,**]

[a] The Key Laboratory for Polymer Processing Engineering of Ministry of Education, National Engineering Research Center of Novel Equipment for Polymer Processing, South China University of Technology, Guangdong, China
[b] Wisconsin Institute for Discovery, University of Wisconsin, Madison, WI, USA
[c] Department of Mechanical Engineering, University of Wisconsin, Madison, WI, USA

ARTICLE INFO

Article history:
Received 13 August 2014
Received in revised form 3 October 2014
Accepted 5 October 2014
Available online 20 October 2014

Keywords:
Poly(propylene carbonate) (PPC)
Chitosan
Electrospinning
Freeze drying
Plasma treatment
Tissue engineering

ABSTRACT

In this study, parallel-aligned poly(propylene carbonate) (PPC) microfibers with a fiber diameter of 1.48 ± 0.42 μm were prepared by electrospinning and modified by oxygen plasma treatment. Next, chitosan nanofibers with a fiber diameter size of 278 ± 98 nm were introduced into the PPC fiber mats by freeze drying. Morphological analyses showed that the PPC scaffolds treated with 0.05 mg/ml chitosan solution provided the best micro and nanofiber structure with abundant chitosan nanofibers but without the formation of films. Surface chemical properties were analyzed by X-ray photoelectron spectroscopy (XPS). The initial water contact angle of the scaffolds decreased from $122.3 \pm 0.4^\circ$ for neat PPC scaffolds to $53.8 \pm 1.6^\circ$ for scaffolds with plasma treatment and chitosan nanofibers. The mechanical properties of the scaffolds were affected by plasma treatment with Young's modulus experiencing a reduction of 63%. Meanwhile, Young's modulus experienced a 26% improvement after the introduction of chitosan nanofibers. Fibroblast cells were cultured on the scaffolds to study the effects of both the plasma treatment and the introduction of chitosan nanofibers on cell adhesion, proliferation, and morphology. The scaffolds with PPC microfibers and chitosan nanofibers showed a superior cell response in terms of cell attachment, cell proliferation, and cell–scaffold interactions over the other scaffolds.

1. Introduction

Tissue engineering is an interdisciplinary field that applies the principles of biology and engineering to develop functional substitutes, such as scaffolds, with or without precursor cells, as medical therapies for damaged tissues (Boland et al., 2006; Pham, Sharma, & Mikos, 2006a). In this field, a highly porous biodegradable scaffold is essential to accommodate mammalian cells and guide their growth in three dimensions. Numerous approaches have been developed to fabricate scaffolds such as gas foaming, solvent casting/particle leaching, thermally induced phase separation, 3D printing, and electrospinning (Hutmacher, 2000). Much attention has been devoted to the electrospinning technique as a fairly accessible processing method that can be used in both synthetic and natural polymers. Electrospinning is a versatile technique that allows the production of fibers with diameters ranging from a few micrometers down to tens of nanometers (Pham et al., 2006a). Moreover, fibers with a particular orientation could be fabricated by modifying the collection device. It has been widely proven that for some types of cells parallel-aligned fibers can direct cell migration, control cell shape, induce cell differentiation, and better mimic the function of the native extracellular matrix (ECM) compared to random fibers (Guex et al., 2012; Mi et al., 2014).

Poly(propylene carbonate) (PPC) is an aliphatic polycarbonate comprised of propylene epoxide and carbon dioxide (CO_2) that was first synthesized in the late 1960s (Inoue, Koinuma, & Tsuruta, 1969). It has recently attracted a lot of attention in the biomedical field due to its good mechanical properties, cytocompatibility, and benign degradation by-products of CO_2 and water (Kim et al., 2008; Luinstra & Borchardt, 2012). These properties make it a competitive candidate for tissue engineering applications (Welle et al., 2007; Zhang et al., 2006, 2007; Zhao, Han, Chen, et al., 2012a). However, the hydrophobicity of PPC has effectively limited its applications in tissue engineering (Jing et al., 2014). It has been generally recognized that the hydrophilicity of a scaffold affects its protein absorption as well as subsequent cell adhesion on the scaffold (Wilson, Clegg, Leavesley, & Pearcy, 2005). When the contact angle of the scaffold is higher than 90°, cells may struggle to attach and proliferate well on the surface of the scaffold (Cui et al., 2012).

* Corresponding author.
** Corresponding author at: Department of Mechanical Engineering, University of Wisconsin, Madison, WI, USA. Tel.: +1 608 316 4310
E-mail addresses: pmxfpeng@scut.edu.cn (X.-F. Peng), turng@engr.wisc.edu, turng@wid.wisc.edu (L.-S. Turng).

http://dx.doi.org/10.1016/j.carbpol.2014.10.025
0144-8617/

A common approach to enhancing the hydrophilicity of biomaterials is surface modification, which can be achieved by plasma treatment. This is a simple and effective method of activating the hydrophilic groups on the surface of biomaterials or further introducing desired chemical groups onto the surface without significantly sacrificing its bulk properties (Chan, Ko, & Hiraoka, 1996; Ibnabddjalil et al., 1994; Wang, Cui, & Bei, 2005). Oxygen containing groups on the surface of the material are formed via plasma treatment, which could improve surface hydrophilicity (Cui & Brown, 2002; Lai et al., 2006; Liston, Martinu, & Wertheimer, 1993). This technique has been widely used in biomedical applications such as tissue culture polystyrene (TCPS) plates used for cell culture study. Alternatively, the addition of hydrophilic synthesized polymers and natural materials has also been widely used to improve scaffold hydrophilicity as well as biocompatibility.

Chitosan has been widely studied as an important tissue engineering material in recent years (Busilacchi, Gigante, Mattioli-Belmonte, Manzotti, & Muzzarelli, 2013; Jana, Florczyk, Leung, & Zhang, 2012; Ji, Annabi, Khademhosseini, & Dehghani, 2011; Levengood & Zhang, 2014; Liu, Wu, Jiao, Xiong, & Zhou, 2013; Ma et al., 2003; Martins et al., 2014; Muzzarelli, Greco, Busilacchi, Sollazzo, & Gigante, 2012). As a unique cationic polysaccharide, chitosan has outstanding biocompatibility, bioadhesion, and biodegradability. There are many methods of introducing chitosan onto synthesized polymers such as alkaline hydrolysis followed by grafting-coating (Lao, Tan, Wang, & Gao, 2008; Sahoo, Sasmal, Nanda, Phani, & Nayak, 2010), layer-by-layer assembly (Zhu, Gao, He, Liu, & Shen, 2003), photo-initiated grafting (Zhu, Zhao, & Ma, 2009), and blending (Cooper, Bhattarai, & Zhang, 2011; Sundaramurthi, Vasanthan, Kuppan, Krishnan, & Sethuraman, 2012). Besides these methods, freeze-drying chitosan solution could also introduce chitosan to the scaffolds (Zhao, Han, Chen, et al., 2012a). The advantage of this method is that the chitosan nanofibers could be introduced deep into the scaffolds rather than on their surfaces only.

There have been controversies surrounding fibrous scaffolds with respect to the optimal fiber diameter for cell culture. Most researchers believe that fibrous scaffolds with fiber diameters of less than 300 nm would be the best for cell growth since they closely mimic the structure of native ECM (Christopherson, Song, & Mao, 2009). However, these small fiber diameters cause small pores and low porosity of the scaffolds, which is a disadvantage for cell penetration and migration (Ju, Choi, Atala, Yoo, & Lee, 2010). Recently, it was reported that fibrous scaffolds with both microfibers and nanofibers showed superior cell affinity than either microfiber scaffolds or nanofiber scaffolds alone (Pham, Sharma & Mikos, 2006b). In addition, it was also found that polylactic acid (PLA) scaffolds with micropores and nanofibril structures showed better properties and cell responses than scaffolds with only micropores (Zhao, Han, Tu, et al., 2012b). Therefore, fabrication of scaffolds with both micro and nanostructures might be a future development direction for tissue engineering scaffolds.

In this study, we prepared parallel-aligned PPC microfibers by electrospinning, treated them with oxygen plasma, and then modified them with chitosan nanofibers by freeze-drying. The aim of this study was to fabricate novel scaffolds with both micro and nanofiber structures, as well as elevated hydrophilicity and biocompatibility, to be suitable for cell adhesion and proliferation.

2. Experimental

2.1. Materials

PPC (QPAC® 40) was purchased from Empower Materials, Inc. Low molecular weight chitosan with a viscosity of 20–300 cP (1 wt% in 1% acetic acid), chloroform (CF, ACS reagent) and N, N-dimethylformamide (DMF, ACS reagent) were purchased from Sigma-Aldrich (Milwaukee, WI, USA). All materials were used as received.

2.2. Fabrication of parallel-aligned PPC microfiber scaffolds

Polymer solutions with a concentration of 10 wt% were prepared by dissolving PPC pellets into the mixed solvents (CF/DMF = 6/4 v/v) and stirring for 12 h at room temperature. The solution was loaded into a 6 ml syringe connected to an 18 gauge blunt needle by Teflon tubing. The desired flow rate was controlled at 0.5 ml/h via a digital syringe pump (Harvard Bioscience Company) and the applied voltage was kept at 18 kV. The parallel alignment was achieved by collecting the electrospun fibers over a gap formed between two parallel conductive copper plates; a setup that was used in our previous study (Mi et al., 2014). Due to the electrostatic interactions, the fibers were oriented by the electric field and stretched to form parallel arrays to cover the gap (Li, Wang, & Xia, 2003, 2004; Wang, Zhao, Turng, & Li, 2013). The electrospun fibers were wrapped on autoclave-sterilized stainless steel washers (inner diameter of 8.33 mm, McMaster–Carr Co.) for cytocompatibility evaluation. The collected electrospun scaffolds were stored in a vacuum oven (Thermo Fisher Scientific, USA) at 40 °C for 24 h to eliminate any possible residual solvents inside of the fibers.

2.3. Preparation of plasma-treated PPC scaffolds and plasma-treated PPC/chitosan hybrid scaffolds

The electrospun scaffolds were treated with oxygen plasma using a plasma etcher (Plasma Etch Inc., Carson, USA) to stimulate the scaffold surface in order to improve the hydrophilicity of the scaffold. The samples were placed in the chamber and treated with oxygen plasma at a pressure of 0.025 mtorr. The radio power generating oxygen plasma was 100 W. The flow rate of oxygen was 50 ml/min and the optimal treatment time was set as 36 s. The plasma-treated PPC scaffolds were named T-PPC in the following study.

Chitosan was dissolved in 0.5% acetic acid at a concentration of 0.03 mg/ml, 0.05 mg/ml, and 0.07 mg/ml, respectively. The plasma-treated scaffolds were immersed into the chitosan solutions for 2 min at room temperature. Then the immersed scaffolds were taken out and placed into liquid nitrogen for 20 min. The frozen scaffolds were freeze dried for 24 h to remove solvents using a freeze dryer (Freezone 4.5, Labconco, USA). The plasma-treated PPC fibers containing chitosan were named T-PPC/CS-3, T-PPC/CS-5, and T-PPC/CS-7 according to their respective chitosan concentration.

2.4. Characterization

2.4.1. Scanning electron microscopy (SEM)

The morphologies of the scaffolds were observed by scanning electron microscopy (SEM) (JEOL, 6500) with an accelerating voltage of 10 kV. Prior to imaging, the specimens were sputtered with gold for 40 s. The fiber orientation angles of the neat PPC fibers were measured from SEM images using the Image J software. The diameters of the PPC microfibers and chitosan nanofibers were measured from SEM images as well using the same software. The fiber orientation angle and fiber diameter distribution were calculated from 50 measurements using three SEM images.

2.4.2. X-ray photoelectron spectroscopy (XPS)

The surface chemistry of the scaffolds was analyzed by X-ray photoelectron spectroscopy (XPS) in order to identify the effect of plasma treatment as well as the involvement of chitosan. The XPS

N 1s core-level signal was used as a marker for the analysis of the chitosan on the surface. XPS measurements were performed on an X-ray photoelectron spectrometer with a focused, monochromatic Kα X-ray source and a monoatomic/cluster ion gun (Thermo Scientific, USA). A survey scan spectrum was taken and surface elemental stoichiometries were determined from peak-area ratios.

2.4.3. Water contact angle (WCA) measurements

To investigate the surface wettability of scaffolds, the water contact angle of the scaffolds was measured by a video contact angle instrument (Dataphysics, OCA 15) using the sessile drop method. Briefly, a drop of water (4 μL) was dropped onto the surface of the scaffolds. The change of the water bead shape was recorded and the surface contact angles were measured at 0, 5, and 10 s. The WCA of each scaffold was the average value of three different spots.

2.4.4. Tensile properties under dry and wet Conditions

The membranes of neat PPC, T-PPC (plasma-treated PPC), and T-PPC/CS (plasma-treated PPC with chitosan), with thickness of about 400 μm, were cut into the same dimensions, $15 \times 10\,mm^2$ (length × width), for better comparison among the specimens. The tensile tests for the dry condition were performed on an Instron 5565 universal testing machine using a 250 N load cell with a crosshead speed of 5 mm/min. The cut specimens were also immersed into phosphate buffered saline (PBS, pH = 7.4) at room temperature for 2 h for the wet condition test. All of the test procedures were the same for both the dry and wet condition tests. At least four samples were tested for each type of scaffold. The ultimate tensile strength, Young's modulus, and elongation-at-break values were obtained from the stress–strain curves.

2.5. Biocompatibility characterization

2.5.1. Cell culture prior to seeding

Swiss mouse NIH 3T3 ECACC (European Collection of Cell Cultures) fibroblasts were used for the biological assays. Cells were cultured in high-glucose Dulbecco's Modified Eagle Medium (DMEM, Invitrogen), supplemented with 20% fetal bovine serum (WiCell), 1 unit/ml penicillin (Invitrogen), 1 μg/ml streptomycin (Invitrogen), and 2 mM L-glutamine (Invitrogen), and maintained on 6-well tissue culture-treated polystyrene (TCPS) plates (BD Falcon) prior to testing. The medium was replaced every two days and cells were passaged with Tryspin-ethylene diaminetetraacetic acid (EDTA) at a 1:40 ratio every 6 days during regular maintenance.

2.5.2. Cell seeding

The scaffolds were exposed to sterilizing Ultra-violet (UV) light for 30 min on each side and placed into 24-well TCPS plates before cell seeding. All cell culture experiments were conducted in 24 well plates that were pre-treated with poly-HEMA to prevent cells attaching to the TCPS plates. The poly-HEMA (Sigma) coating was prepared by 2% poly-HEMA solution in 100% ethanol. 3T3 cells were dissociated with Tryspin-EDTA for 5 min prior to seeding. The cells were then seeded onto the sterilized scaffolds at a density of 40,000 cells/well in the high-glucose 3T3 medium. The medium was replaced every 2 days.

2.5.3. Cell attachment and cell viability

To quantify the cell attachment onto the scaffolds, after 12 h, the incubation medium was aspirated and the cells were washed with PBS twice, fixed with 4% paraformaldehyde (PFA) diluted in PBS, and incubated in 0.05% 4′,6-diamidino-2-phenylindole (DAPI) in PBS for 5 min at 37 °C. A Nikon Eclipse Ti microscope was used to image the cells and the number of attached cells were counted using Image J software. Six locations on each scaffold were imaged and three samples were used to obtain the cell number.

To confirm the viability of cells cultured on the chosen scaffolds, cells were stained with a Live/Dead Viability/Cytotoxicity kit (Invitrogen). Cell viability was determined 3 days and 10 days after seeding. This kit provided an assay to simultaneously visualize both live and dead cells. The stain utilized green fluorescent Calcein-AM to target esterase activity within the cytoplasm of living cells, and red fluorescent ethidium homodimer-1 (EthD-1) to indicate cell death by penetrating damaged cellular membranes. A Nikon Eclipse Ti microscope was used to image the cells.

2.5.4. Cell proliferation

To study the cell proliferation on different scaffolds, the cells cultured on the scaffolds were initially washed twice with PBS to ensure that the cells collected were not growing in suspension within the poly-HEMA coated plates. TrypLE (Life Technologies) was then used for 5 min at 37 °C to detach the cells. After incubation, the cells were collected and centrifuged at 200 rpm for 5 min. The supernatant was then aspirated and the cells resuspended in 600 μL of PBS and filtered prior to analysis. Data was acquired with an Accuri C6 flow cytometer (BD Biosciences).

2.5.5. Cytoskeleton study

The cytoskeleton organization of the cells was determined by phalloidin–tetramethylrhodamine B isothiocyanate (phalloidin–TMRho, Sigma) staining. For these assays, after 3 days culture, cells were first washed with PBS twice and then fixed in 4% PFA diluted in PBS for 15 min at room temperature. Cells were then washed with PBS and permeabilized with 1% Triton-X in PBS for 6 min at room temperature. The cells were washed with PBS again and treated with 0.3 μM phalloidin–TMRho with DAPI for 1 h at room temperature. Samples were then washed with PBS and imaged using a Nikon Eclipse Ti microscope.

2.5.6. Statistical analysis

All of the quantitative results were expressed as mean ± standard deviation (SD). Statistical analyses were carried out by means of a one-way analysis of variance (ANOVA). The difference between factors was analyzed by a Tukey test. A p-value less than 0.05 and 0.01 were considered statistically significant.

3. Results and discussion

3.1. Morphology of electrospun and treated PPC fibers

The SEM micrographs of untreated and plasma-treated electrospun aligned PPC fibers are shown in Fig. 1. The original electrospun PPC fibers are smooth and bead-less, and 95% fibers aligned within ±20° of the alignment direction (Fig. 1(a) and (b)). Moreover, after plasma treatment, the surface of the fibers became rougher with the appearance of more and larger cracks (Fig. 1(c)) compared to the untreated fibers (Fig. 1(d)). Fig. 2 shows the morphology of T-PPC/CS with different chitosan concentrations. As can be seen in Fig. 2(a), very few chitosan nanofibers were detected on the surface of the T-PPC/CS-3 scaffold, with the amount of chitosan nanofibers increasing at increased chitosan concentrations. The best results were obtained when the chitosan concentration was 0.05 mg/ml (Fig. 2(b)), at which the fiber diameter of PPC microfibers ranged from 0.8 to2.8 μm with the average value of 1.48 ± 0.42 μm, and the average diameter of the chitosan nanofibers was 278.56 ± 98.51 nm, with fiber diameters ranging from 100 to 600 nm, as shown in Fig. 2(e) and (f) respectively. When the chitosan concentration further increased, some chitosan films were formed besides the nanofibers and covered the fibrous structure of the electrospun PPC (Fig. 2(c)). For comparison, untreated PPC fibers were also freeze dried with the chitosan solution (0.05 mg/ml) as shown in Fig. 2(d). However, it

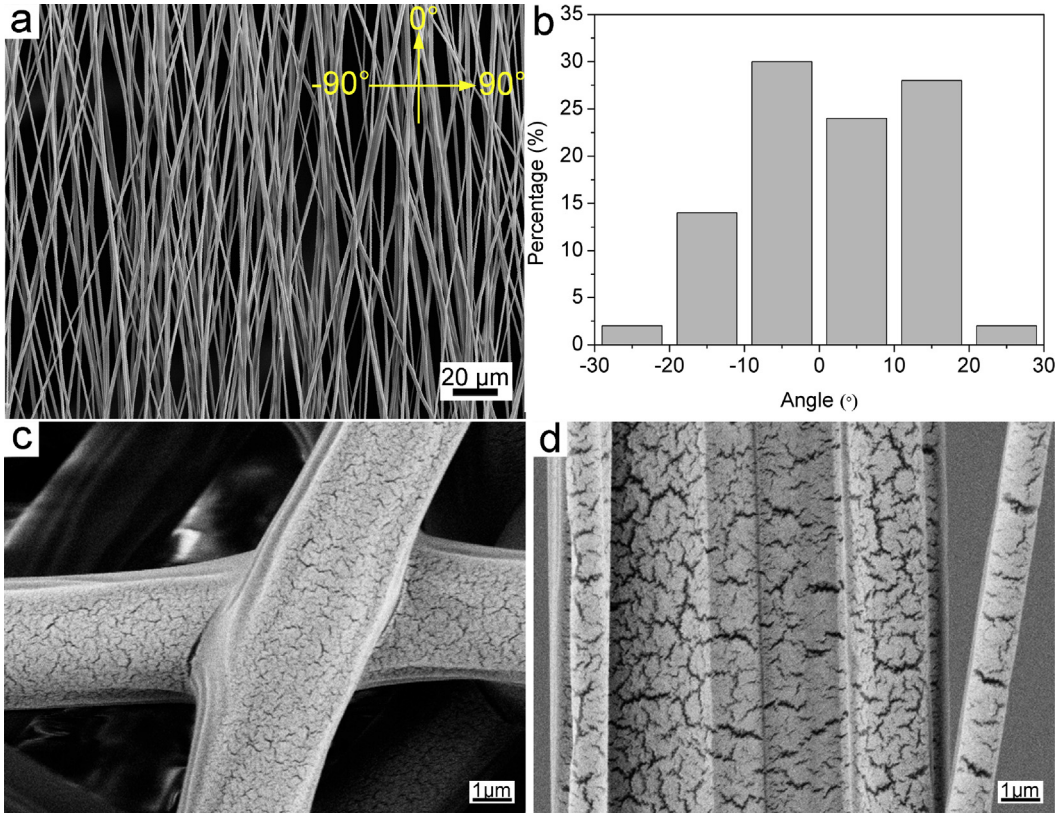

Fig. 1. SEM micrographs of untreated and plasma-treated PPC microfibers: (a) untreated electrospun PPC fibers, (b) fiber orientation angles of aligned fibers, (c) morphology of the untreated fiber surface, and (d) morphology of the plasma-treated fiber surface.

was found that very few chitosan nanofibers were introduced, far less than those on the plasma-treated PPC scaffolds (Fig. 2(b)).

These results indicated that the oxygen plasma treatment affected the presence of chitosan nanofibers on the electrospun PPC fibers. This might have been because the PPC fibers after plasma treatment exhibited higher wettability leading to more chitosan solution absorption as compared to the untreated PPC fibers. Therefore, more chitosan nanofibers were introduced on the plasma-treated PPC fibers afterwards. The incorporation of chitosan with synthetic polymer scaffolds has shown significant advantages in improving scaffold biocompatibility. It has been discovered that gradient CS/PCL electrospun scaffolds prepared by the co-electrospinning technique were more favorable for endothelial cell growth than uniform CS/PCL nanofibers (Du et al., 2012). Moreover, it has been reported that scaffolds with both micro and nanostructures were favorable for cell growth. For example, electrospun PCL scaffolds at suitable thicknesses with multilayer nanofiber/microfiber structures could influence rat marrow

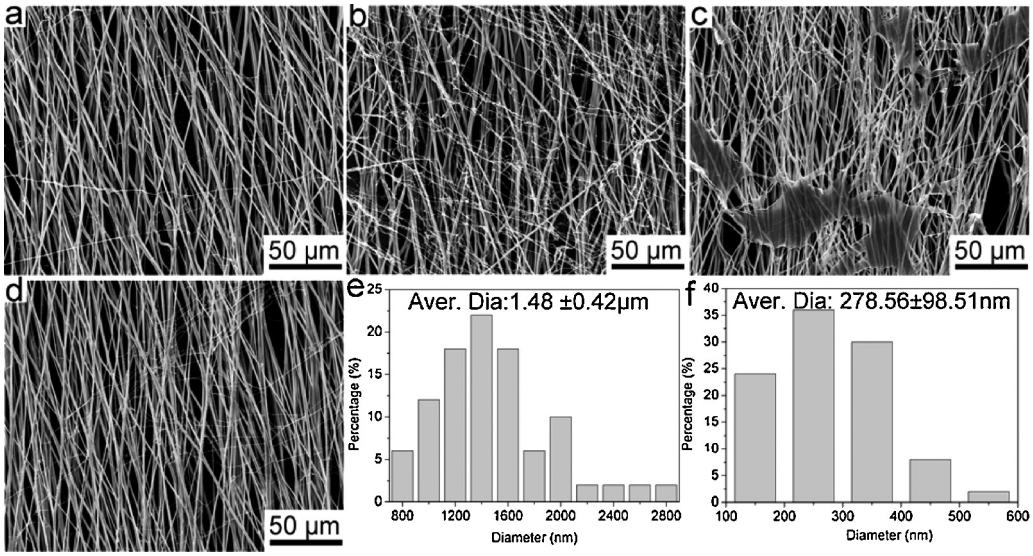

Fig. 2. SEM images of plasma-treated PPC/chitosan hybrid scaffolds: (a) T-PPC/CS-3, (b) T-PPC/CS-5, (c) T-PPC/CS-7, (d) PPC/CS-5, (e) fiber diameter range of PPC microfibers, and (f) fiber diameter range of chitosan nanofibers.

stromal cell attachment, spreading, and infiltration (Pham et al., 2006b). Therefore, it is expected that the involvement of chitosan nanofibers in PPC microfibers could improve the scaffold biocompatibility as well as the structural affinity to cells. Since the scaffolds with 0.05 mg/ml chitosan solution showed the best morphological results, these scaffolds were used to do the following studies and the name of these scaffolds was abbreviated as T-PPC/CS.

3.2. Chemical composition of the scaffolds

XPS was used to analyze the surface chemistry of electrospun PPC, T-PPC, and T-PPC/CS scaffolds. According to the chemical structure of PPC, XPS analysis of the PPC scaffolds indicated that the surface was dominated by carbon and oxygen. Generally, the elemental composition of plasma-treated samples would change due to surface oxidation. High-resolution peak analysis of carbon 1s was performed on the three groups of scaffolds to detect the chemical functional groups present at the surface. As shown in Fig. 3(a) and (b), three components of C 1s core level peak were exhibited in the PPC and T-PPC scaffolds, corresponding to the aliphatic carbon bonds (C—C), carbon single bonded to oxygen (C—O), and carboxyl functional groups (C═O) located at about 284, 286, and 289 eV, respectively. Based on previous reports, plasma-induced polar groups such as oxygen-containing groups tend to increase and thus enhance the hydrophilic behavior of polymers (Cui & Brown, 2002; Lai et al., 2006; Lianos, Quet, & Duc, 1994; Liston et al., 1993; Martins et al., 2009). As was expected, the content of oxygen-containing groups (e.g., C—O and C═O) increased after plasma treatment (Fig. 3(b)). For the T-PPC/CS scaffold, a third peak belonging to nitrogen from amino groups was detected in the whole survey scans, besides the two main components of carbon and oxygen, which verified the existence of chitosan in the scaffold (Fig. 3(c)). The C—N bond was also separated from the C 1s core level peak; its content was about 8.5%. Hence, the XPS analyses confirmed that the plasma treatment and the freeze dried chitosan led to different surface chemistries, which in turn affected wettability, and consequently, cell attachment.

3.3. Surface wettability of the scaffolds

Water contact angles reflect the hydrophilicity of the scaffolds, which affect protein absorption and subsequent cell adhesion on the scaffolds. Hence, contact angle measurements were carried out on PPC, T-PPC and T-PPC/CS to investigate the effects of plasma treatment, as well as the involvement of chitosan, on surface hydrophilicity. The results are shown in Fig. 4. It was demonstrated that neat PPC scaffolds were hydrophobic with a water contact angle higher than 110° and the angle did not change very much during the 10 s recording. However, after plasma treatment, the initial water contact angle decreased from $122.3 \pm 0.4°$ to $91.4 \pm 2.1°$. Furthermore, the sample showed a water contact angle of $53.8 \pm 1.6°$ after introducing chitosan nanofibers. In addition, the water contact angles of T-PPC and T-PPC/CS scaffolds decreased to 0° within 10 s. These results suggested that plasma treatment and chitosan nanofiber introduction could significantly enhance scaffold hydrophilicity. These improvements should be helpful for cell adhesion and proliferation.

3.4. Mechanical properties of the scaffolds

The mechanical properties of the PPC, T-PPC and T-PPC/CS scaffolds were characterized by tensile tests; the results are shown in Fig. 5 and summarized in Table 1. At both dry and wet conditions, the PPC scaffolds showed the highest mechanical properties

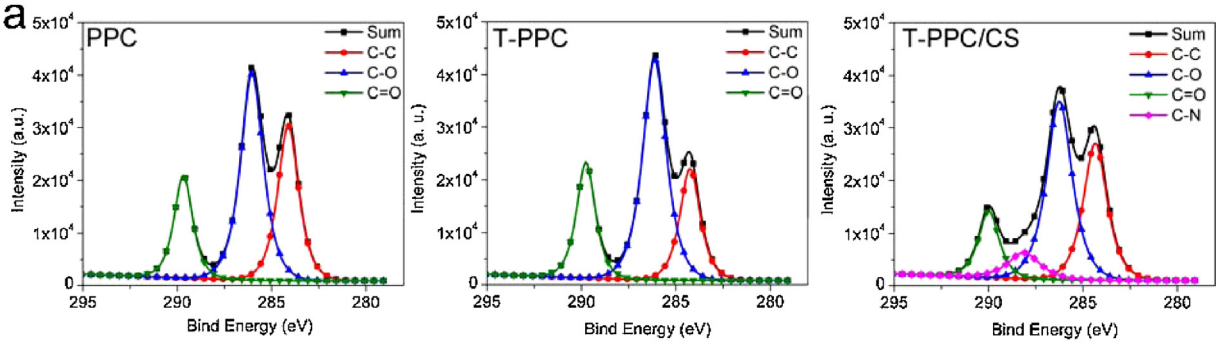

Fig. 3. (a) High resolution C 1s core level signals of PPC, T-PPC, and T-PPC/CS scaffolds. (b) Functional group compositions of PPC, T-PPC, and T-PPC/CS scaffolds. (c) The whole survey scans of PPC, T-PPC, and T-PPC/CS scaffolds.

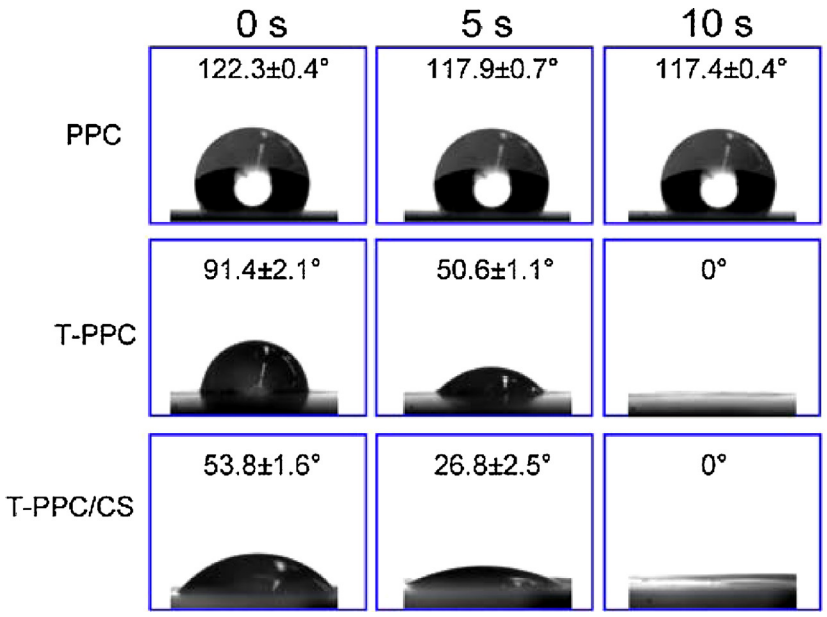

Fig. 4. Water contact angle values of PPC, T-PPC, and T-PPC/CS scaffolds at 0, 5, and 10 s.

Table 1
Tensile test statistical results of PPC, T-PPC, and T-PPC/CS scaffolds at dry and wet conditions presented as average ± standard deviation.

	Dry			Wet		
	Tensile strength (MPa)	Young's modulus (MPa)	Elongation at break (%)	Tensile strength (MPa)	Young's modulus (MPa)	Elongation at break (%)
PPC	7.2 ± 1.0	429.6 ± 55.4	191.3 ± 32.3	6.9 ± 1.2	419.9 ± 51.2	202.1 ± 23.6
T-PPC	4.0 ± 0.9	153.9 ± 36.3	201.3 ± 19.9	3.8 ± 0.3	122.6 ± 5.6	204.6 ± 34.9
T-PPC/CS	5.0 ± 0.8	193.2 ± 34.5	210.7 ± 36.0	4.5 ± 0.4	128.4 ± 5.2	227.3 ± 28.1

followed by T-PPC/CS and T-PPC. This means that the plasma treatment caused the breakage of some chemical bonds of PPC in order to introduce oxygen bonds, which led to a reduction of mechanical properties (recall from Fig. 1(d) that cracks on the fiber surface increased after plasma treatment). The mechanical properties of T-PPC/CS were higher than T-PPC under dry conditions, while the difference was not obvious under wet conditions. This is because the chitosan nanofibers provided additional strength to the scaffold under dry conditions, while this effect disappeared once the chitosan nanofibers were hydrated. Overall, the scaffolds tested under wet conditions showed inferior mechanical properties to those tested under dry conditions due to the plasticizing effect of water. The reduction of mechanical properties of PPC scaffolds in the wet conditions was not very significant due to its hydrophobicity. Although the plasma treatment caused a reduction of mechanical strength in the scaffolds, the mechanical properties of the treated scaffolds were still comparable to many human tissues, such as cancellous bone and cartilage, for which the tensile strength and Young's modulus are about 5 MPa and 50–100 MPa for cancellous bone, and 4 MPa and 15 MPa for cartilage, respectively (Mi et al., 2013). Therefore, the T-PPC/CS scaffolds prepared here have the potential to be used for many tissue applications.

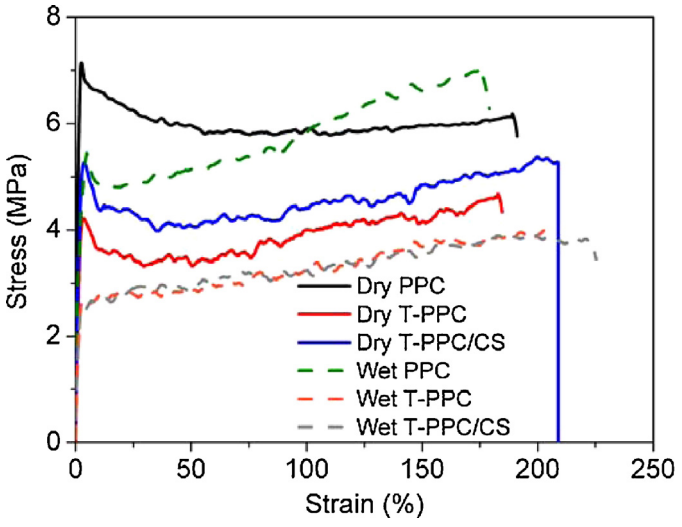

Fig. 5. Representative stress–strain curves for PPC, T-PPC, and T-PPC/CS scaffolds under dry and wet conditions.

3.5. Cell viability and proliferation

Cell attachment on the scaffolds was investigated by staining the cell nucleus using DAPI. Fig. 6 shows the quantitative analysis results of cell attachment and the fluorescent microscopic images of cells on the scaffolds. It was found that the cell attachment on T-PPC scaffolds was higher than that of PPC scaffolds, while it was lower than that of T-PPC/CS scaffolds. This might have been due to the plasma treatment changed the surface wettability of the scaffolds by incorporating oxygen-containing groups. The presence of chitosan on the T-PPC/CS scaffolds facilitated cell attachment by providing additional hydrophilic amino groups. The enhanced wettability of the scaffolds might have been relevant to the absorption of serum-derived proteins, which could have further influenced cell attachment by changing the interactions between the cells and the scaffolds (Baker et al., 2006; Lai et al., 2006).

The cell viability results are shown in Figs. 7 and 8(a). Consistent with the cell attachment results, the cell viability on the T-PPC and T-PPC/CS scaffolds was enhanced. The cells were found

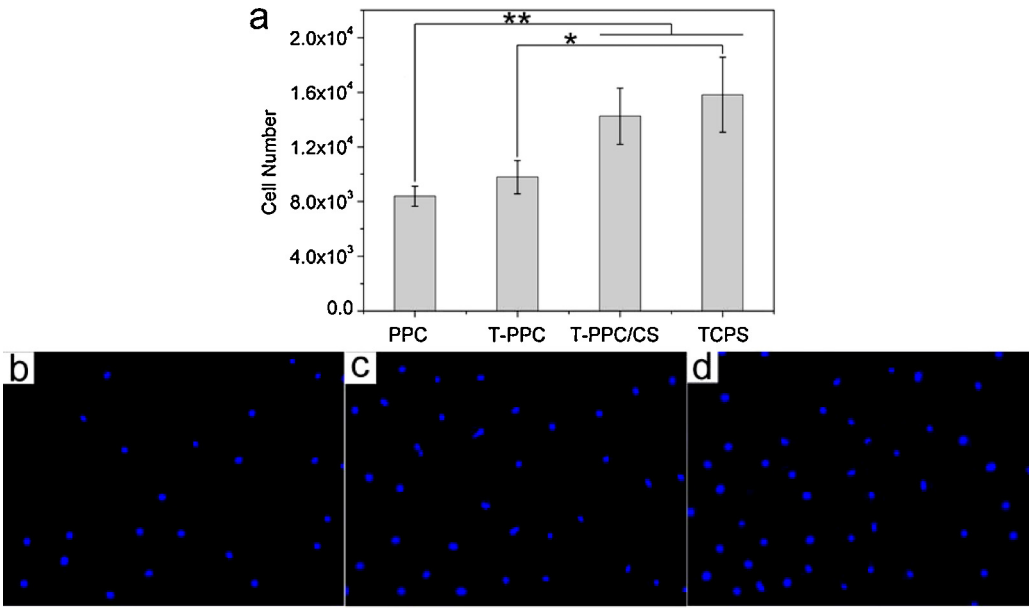

Fig. 6. (a) Cell attachment statistical results of PPC, T-PPC, and T-PPC/CS scaffolds after 4 h seeding. DAPI staining of 3T3 cells on (b) PPC scaffold, (c) T-PPC scaffold, and (d) T-PPC/CS scaffold.

to grow towards one direction on the scaffolds because of the parallel-aligned PPC microfibers. Most cells showed spindle-like shapes on the T-PPC/CS scaffolds after 3 days and 10 days culture, demonstrating a flourishing living state of fibroblast cells. This might be attributable to the improved biocompatibility by chitosan nanofibers on the scaffolds (Skotak, Leonov, Larsen, Noriega, & Subramanian, 2008). In addition, it was found that the average cell viability of all scaffolds was higher than 85% after 10 days of culture. Moreover, it should be noted that the T-PPC/CS scaffolds had an average 95% live cells at day 3 and an average 98% live cells at day 10 indicating good biocompatibility of the scaffolds. Fig. 8(b) shows the cell proliferation results after 3 days and 10 days culture. Cell proliferation was found to increase with culture time, similar to the trend observed on TCPS (control) (Prabhakaran, Kai, Ghasemi-Mobarakeh, & Ramakrishna, 2011). At day 3 and day 10, T-PPC/CS showed the highest cell population followed by T-PPC scaffolds and neat PPC scaffolds. The difference between T-PPC/CS and PPC scaffolds was statistically significant. These results agreed with cell attachment and cell viability tests which further proved that plasma treatment and the involvement of chitosan nanofibers in the electrospun PPC microfibers were favorable for cell attachment, survival, and proliferation.

3.6. Cytoskeleton study

The cell morphology was examined by culturing the 3T3 fibroblast cells on the scaffolds for 3 days then stained with phalloidin to gain a better understanding of the cellular response to the scaffolds. Overall, the cells migrated in one direction which was the same as the PPC fiber alignment direction. Furthermore, some cells showed an elongated shape in this direction. The presence of chitosan nanofibers in the T-PPC/CS scaffolds did not have any adverse

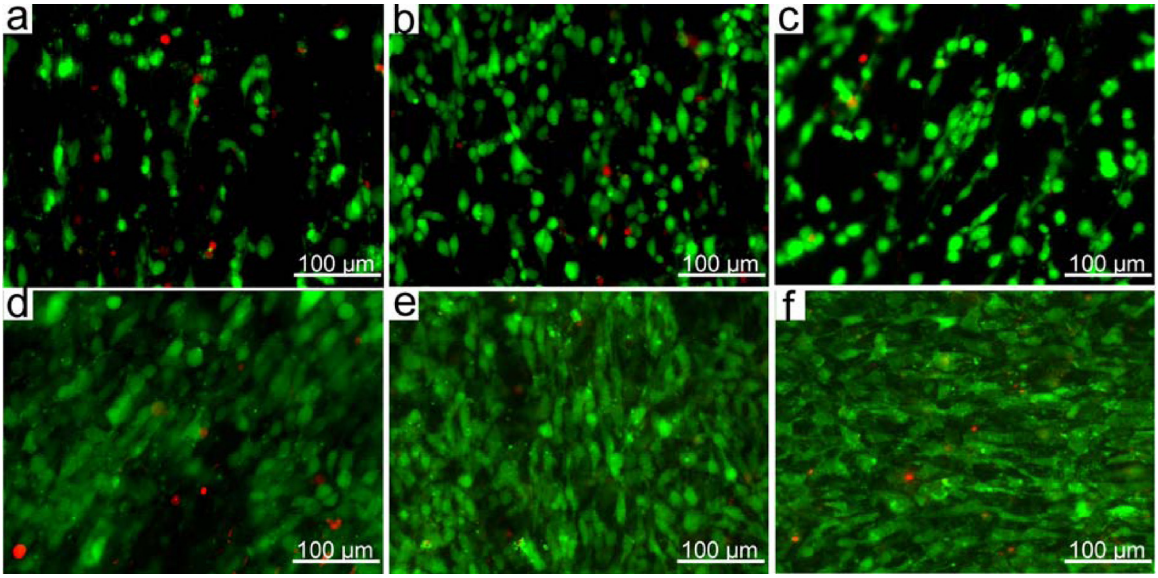

Fig. 7. Day 3 and Day 10 live/dead assays showing 3T3 fibroblast cells cultured on (a, d) PPC, (b, e) T-PPC, and (c, f) T-PPC/CS scaffolds. Live cells showed green fluorescence and dead cells were indicated by red fluorescence (the images on the first and second rows are the results on Days 3 and 10, respectively).

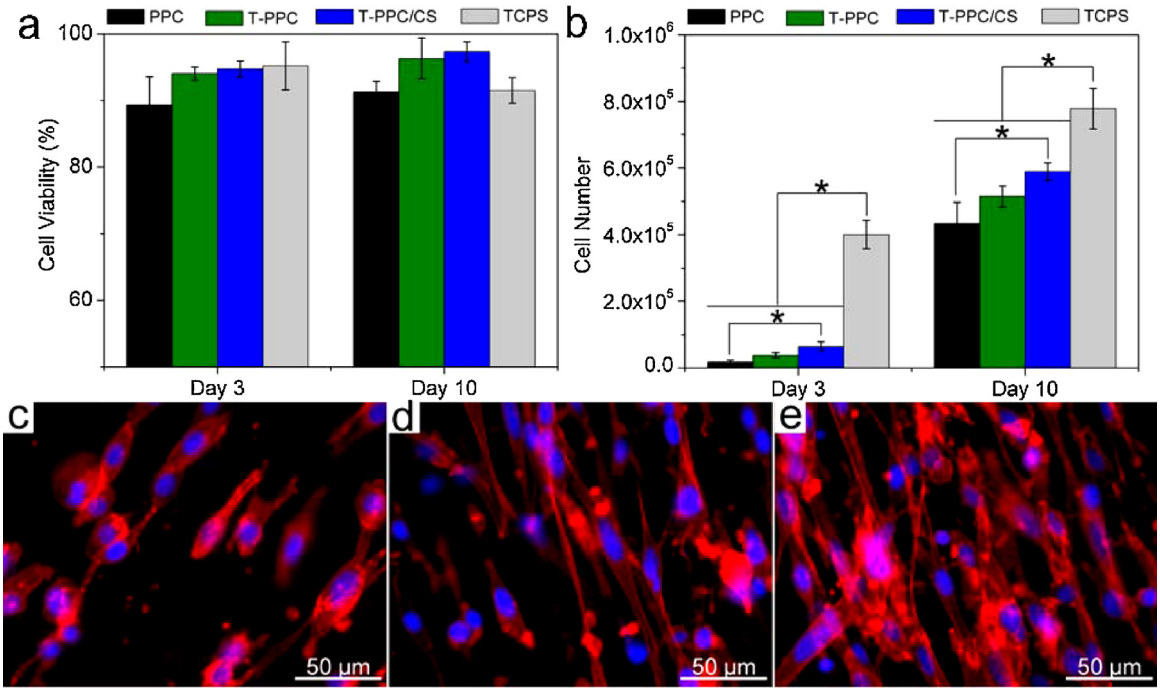

Fig. 8. (a) Cell viability statistical results of 3T3 fibroblast cells cultured on PPC, T-PPC, and T-PPC/CS scaffolds. (b) Cell proliferation statistical results of 3T3 fibroblast cells cultured on PPC, T-PPC, and T-PPC/CS scaffolds at Day 3 and Day 10 time points. Cytoskeleton study of 3T3 fibroblast cells cultured on (c) PPC, (d) T-PPC, and (e) T-PPC/CS scaffolds after 3 days of culture.

effects on cell alignment. In particular, it was found that cells on the T-PPC and T-PPC/CS scaffolds presented a spindle shape, especially on the T-PPC/CS scaffolds where cells showed obvious extended pseudopodia of filaments, indicating that there were good interactions between the cells and the scaffolds. On the other hand, cells on the PPC scaffolds were more elliptical, without showing clear pseudopodia (Fig. 8(c)). In contrast, cells on T-PPC and T-PPC/CS scaffolds were more stretched out, and some cell nuclei were elongated along the cell spreading direction (shown in Fig 8(d) and (e)). It is likely that cell adhesion was more limited on the neat PPC scaffolds due to the hydrophobicity of the scaffolds and the cells could not migrate freely, which resulted in lower cytoskeleton tension. The hydrophilicity of the T-PPC and T-PPC/CS scaffolds facilitated the adsorption of fibronectin or vitronectin proteins (Yildirim et al., 2010), which further enhanced the cell adhesion and led to the presence of cell pseudopodia. Chen et al. also found that plasma treated poly(l-lactide) scaffolds were more favorable for endothelial and smooth muscle cell growth (Cheng, Lee, Komvopoulos, Yan, & Li, 2013). After introducing chitosan nanofibers, the actin bundles of the cells were more obvious and the cells were more stretched out, demonstrating that the cells flourished more on the T-PPC/CS scaffolds. It has been reported that chitosan provided a microenvironment with favorable physicochemical properties for cell adhesion and proliferation (Dang & Leong, 2006; Lee, Jeong, Kang, Lee, & Park, 2009). The advantages of chitosan nanofibers in electrospun parallel-aligned PPC microfibers were proved in our present study as well.

4. Conclusions

In this study, electrospun parallel-aligned PPC microfibers were treated with oxygen plasma and chitosan nanofibers were introduced by freeze drying in order to develop novel tissue engineering scaffolds with both micro and nanofiber structures, as well as high biocompatibility and favorable cellular responses. It was found that electrospun PPC microfibers could achieve 95% of fibers aligned within ±20°, with average fiber diameters of 1.48 ± 0.42 μm. The 0.05 mg/ml chitosan solution provided the best nanofiber structure, with an average chitosan nanofiber diameter of 278.56 ± 98.51 nm. This fibrous scaffold contains both micro and nano fibers has the similar structure of native ECM. The plasma treatment on the scaffolds led to higher water contact angles, and the addition of chitosan nanofibers further improved scaffold hydrophilicity. Although plasma treatment caused a reduction in scaffold mechanical properties, the scaffolds were still capable of many tissue applications. 3T3 fibroblast cell culture results suggested that the plasma treated and chitosan-incorporated T-PPC/CS scaffolds showed the highest cell adhesion, cell viability, and cell proliferation as compared to neat PPC and plasma treated T-PPC scaffolds. Moreover, the cells on the T-PPC/CS scaffolds flourished, showing typical spindle shapes and extended pseudopodia.

Acknowledgments

The authors would like to acknowledge the support of the Wisconsin Institute for Discovery (WID), the China Scholarship Council, the financial support of the National Nature Science Foundation of China (no. 51073061, no. 21174044), the Guangdong Nature Science Foundation (no. S2013020013855, no. 9151064101000066), and the National Basic Research Development Program 973 (no. 2012CB025902) of China.

References

Baker, S. C., Atkin, N., Gunning, P. A., Granville, N., Wilson, K., Wilson, D., et al. (2006). Characterisation of electrospun polystyrene scaffolds for three-dimensional in vitro biological studies. *Biomaterials*, *27*(16), 3136–3146.

Boland, E. D., Pawlowski, K. J., Barnes, C. P., Simpson, D. G., Wnek, G. E., & Bowlin, G. L. (2006). Electrospinning of bioresorbable polymers for tissue engineering scaffolds. *Polymeric Nanofibers*, *918*, 188–204.

Busilacchi, A., Gigante, A., Mattioli-Belmonte, M., Manzotti, S., & Muzzarelli, R. A. A. (2013). Chitosan stabilizes platelet growth factors and modulates stem cell differentiation toward tissue regeneration. *Carbohydrate Polymers*, *98*(1), 665–676.

Chan, C. M., Ko, T. M., & Hiraoka, H. (1996). Polymer surface modification by plasmas and photons. *Surface Science Reports*, *24*(1–2), 3–54.

Cheng, Q., Lee, B. L. P., Komvopoulos, K., Yan, Z. Q., & Li, S. (2013). Plasma surface chemical treatment of electrospun poly(L-Lactide) microfibrous scaffolds for enhanced cell adhesion, growth, and infiltration. *Tissue Engineering Part A*, *19*(9–10), 1188–1198.

Christopherson, G. T., Song, H., & Mao, H. Q. (2009). The influence of fiber diameter of electrospun substrates on neural stem cell differentiation and proliferation. *Biomaterials*, *30*(4), 556–564.

Cooper, A., Bhattarai, N., & Zhang, M. Q. (2011). Fabrication and cellular compatibility of aligned chitosan-PCL fibers for nerve tissue regeneration. *Carbohydrate Polymers*, *85*(1), 149–156.

Cui, N. Y., & Brown, N. M. D. (2002). Modification of the surface properties of a polypropylene (PP) film using an air dielectric barrier discharge plasma. *Applied Surface Science*, *189*(1–2), 31–38.

Cui, W. G., Cheng, L. Y., Li, H. Y., Zhou, Y., Zhang, Y. G., & Chang, J. (2012). Preparation of hydrophilic poly(L-lactide) electrospun fibrous scaffolds modified with chitosan for enhanced cell biocompatibility. *Polymer*, *53*(11), 2298–2305.

Dang, J. M., & Leong, K. W. (2006). Natural polymers for gene delivery and tissue engineering. *Advanced Drug Delivery Reviews*, *58*(4), 487–499.

Du, F. Y., Wang, H., Zhao, W., Li, D., Kong, D. L., Yang, J., et al. (2012). Gradient nanofibrous chitosan/poly epsilon-caprolactone scaffolds as extracellular microenvironments for vascular tissue engineering. *Biomaterials*, *33*(3), 762–770.

Guex, A. G., Kocher, F. M., Fortunato, G., Korner, E., Hegemann, D., Carrel, T. P., et al. (2012). Fine-tuning of substrate architecture and surface chemistry promotes muscle tissue development. *Acta Biomaterialia*, *8*(4), 1481–1489.

Hutmacher, D. W. (2000). Scaffolds in tissue engineering bone and cartilage. *Biomaterials*, *21*(24), 2529–2543.

Ibnabddjalil, M., Loh, I. H., Chu, C. C., Blumenthal, N., Alexander, H., & Turner, D. (1994). Effect of surface plasma treatment on the chemical, physical, morphological, and mechanical-properties of totally absorbable bone internal-fixation devices. *Journal of Biomedical Materials Research*, *28*(3), 289–301.

Inoue, S., Koinuma, H., & Tsuruta, T. (1969). Copolymerization of carbon dioxide and epoxide. *Journal of Polymer Science Part B—Polymer Letters*, *7*(4), 287–292.

Jana, S., Florczyk, S. J., Leung, M., & Zhang, M. Q. (2012). High-strength pristine porous chitosan scaffolds for tissue engineering. *Journal of Materials Chemistry*, *22*(13), 6291–6299.

Ji, C. D., Annabi, N., Khademhosseini, A., & Dehghani, F. (2011). Fabrication of porous chitosan scaffolds for soft tissue engineering using dense gas CO_2. *Acta Biomaterialia*, *7*(4), 1653–1664.

Jing, X., Salick, M. R., Cordie, T., Mi, H. Y., Peng, X. F., & Turng, L. S. (2014). Electrospinning homogeneous nanofibrous poly(propylene carbonate)/gelatin composite scaffolds for tissue engineering. *Industrial and Engineering Chemistry Research*, *53*(22), 9391–9400.

Ju, Y. M., Choi, J. S., Atala, A., Yoo, J. J., & Lee, S. J. (2010). Bilayered scaffold for engineering cellularized blood vessels. *Biomaterials*, *31*(15), 4313–4321.

Kim, G., Ree, M., Kim, H., Kim, I. J., Kim, J. R., & Lee, J. I. (2008). Biological affinity and biodegradability of poly(propylene carbonate) prepared from copolymerization of carbon dioxide with propylene oxide. *Macromolecular Research*, *16*(5), 473–480.

Lai, J. N., Sunderland, B., Xue, J. M., Yan, S., Zhao, W. J., Folkard, M., et al. (2006). Study on hydrophilicity of polymer surfaces improved by plasma treatment. *Applied Surface Science*, *252*(10), 3375–3379.

Lao, L. H., Tan, H. P., Wang, Y. J., & Gao, C. Y. (2008). Chitosan modified poly(L-lactide) microspheres as cell microcarriers for cartilage tissue engineering. *Colloids and Surfaces B—Biointerfaces*, *66*(2), 218–225.

Lee, K. Y., Jeong, L., Kang, Y. O., Lee, S. J., & Park, W. H. (2009). Electrospinning of polysaccharides for regenerative medicine. *Advanced Drug Delivery Reviews*, *61*(12), 1020–1032.

Levengood, S. K. L., & Zhang, M. Q. (2014). Chitosan-based scaffolds for bone tissue engineering. *Journal of Materials Chemistry B*, *2*(21), 3161–3184.

Li, D., Wang, Y. L., & Xia, Y. N. (2003). Electrospinning of polymeric and ceramic nanofibers as uniaxially aligned arrays. *Nano Letters*, *3*(8), 1167–1171.

Li, D., Wang, Y. L., & Xia, Y. N. (2004). Electrospinning nanofibers as uniaxially aligned arrays and layer-by-layer stacked films. *Advanced Materials*, *16*(4), 361–366.

Lianos, L., Quet, C., & Duc, T. M. (1994). Surface structural studies of polyethylene, polypropylene and their copolymers with tof sims. *Surface and Interface Analysis*, *21*(1), 14–22.

Liston, E. M., Martinu, L., & Wertheimer, M. R. (1993). Plasma surface modification of polymers for improved adhesion—A critical-review. *Journal of Adhesion Science and Technology*, *7*(10), 1091–1127.

Liu, M. X., Wu, C. C., Jiao, Y. P., Xiong, S., & Zhou, C. R. (2013). Chitosan-halloysite nanotubes nanocomposite scaffolds for tissue engineering. *Journal of Materials Chemistry B*, *1*(15), 2078–2089.

Luinstra, G. A., & Borchardt, E. (2012). Material properties of poly(propylene carbonates). *Synthetic Biodegradable Polymers*, *245*, 29–48.

Ma, L., Gao, C. Y., Mao, Z. W., Zhou, J., Shen, J. C., Hu, X. Q., et al. (2003). Collagen/chitosan porous scaffolds with improved biostability for skin tissue engineering. *Biomaterials*, *24*(26), 4833–4841.

Martins, A., Pinho, E. D., Faria, S., Pashkuleva, I., Marques, A. P., Reis, R. L., et al. (2009). Surface modification of electrospun polycaprolactone nanofiber meshes by plasma treatment to enhance biological performance. *Small*, *5*(10), 1195–1206.

Martins, A. M., Eng, G., Caridade, S. G., Mano, J. F., Reis, R. L., & Vunjak-Novakovic, G. (2014). Electrically conductive chitosan/carbon scaffolds for cardiac tissue engineering. *Biomacromolecules*, *15*(2), 635–643.

Mi, H. Y., Salick, M. R., Jing, X., Crone, W. C., Peng, X. F., & Turng, L. S. (2014). Electrospinning of unidirectionally and orthogonally aligned thermoplastic polyurethane nanofibers: Fiber orientation and cell migration. *Journal of Biomedical Materials Research Part A*, *00A*.

Mi, H. Y., Salick, M. R., Jing, X., Jacques, R. B., Crone, W. C., Peng, X. F., et al. (2013). Characterization of thermoplastic polyurethane/polylactic acid (TPU/PLA) tissue engineering scaffolds fabricated by microcellular injection molding. *Materials Science and Engineering: C*, *33*(8), 4767–4776.

Muzzarelli, R. A. A., Greco, F., Busilacchi, A., Sollazzo, V., & Gigante, A. (2012). Chitosan, hyaluronan and chondroitin sulfate in tissue engineering for cartilage regeneration: A review. *Carbohydrate Polymers*, *89*(3), 723–739.

Pham, Q. P., Sharma, U., & Mikos, A. G. (2006a). Electrospinning of polymeric nanofibers for tissue engineering applications: A review. *Tissue Engineering*, *12*(5), 1197–1211.

Pham, Q. P., Sharma, U., & Mikos, A. G. (2006b). Electrospun poly(epsilon–caprolactone) microfiber and multilayer nanofiber/microfiber scaffolds: Characterization of scaffolds and measurement of cellular infiltration. *Biomacromolecules*, *7*(10), 2796–2805.

Prabhakaran, M. P., Kai, D., Ghasemi-Mobarakeh, L., & Ramakrishna, S. (2011). Electrospun biocomposite nanofibrous patch for cardiac tissue engineering. *Biomedical Materials*, *6*(5), 55–67.

Sahoo, S., Sasmal, A., Nanda, R., Phani, A. R., & Nayak, P. L. (2010). Synthesis of chitosan–polycaprolactone blend for control delivery of ofloxacin drug. *Carbohydrate Polymers*, *79*(1), 106–113.

Skotak, M., Leonov, A. P., Larsen, G., Noriega, S., & Subramanian, A. (2008). Biocompatible and biodegradable ultrafine fibrillar scaffold materials for tissue engineering by facile grafting of L-lactide onto chitosan. *Biomacromolecules*, *9*(7), 1902–1908.

Sundaramurthi, D., Vasanthan, K. S., Kuppan, P., Krishnan, U. M., & Sethuraman, S. (2012). Electrospun nanostructured chitosan-poly(vinyl alcohol) scaffolds: A biomimetic extracellular matrix as dermal substitute. *Biomedical Materials*, *7*(4), 45005–45017.

Wang, S. G., Cui, W. J., & Bei, J. Z. (2005). Bulk and surface modifications of polylactide. *Analytical and Bioanalytical Chemistry*, *381*(3), 547–556.

Wang, X. F., Zhao, H. B., Turng, L. S., & Li, Q. (2013). Crystalline morphology of electrospun poly(epsilon–caprolactone) (PCL) nanofibers. *Industrial and Engineering Chemistry Research*, *52*(13), 4939–4949.

Welle, A., Kroger, M., Doring, M., Niederer, K., Pindel, E., & Chronakis, I. S. (2007). Electrospun aliphatic polycarbonates as tailored tissue scaffold materials. *Biomaterials*, *28*(13), 2211–2219.

Wilson, C. J., Clegg, R. E., Leavesley, D. I., & Pearcy, M. J. (2005). Mediation of biomaterial-cell interactions by adsorbed proteins: A review. *Tissue Engineering*, *11*(1–2), 1–18.

Yildirim, E. D., Besunder, R., Pappas, D., Allen, F., Guceri, S., & Sun, W. (2010). Accelerated differentiation of osteoblast cells on polycaprolactone scaffolds driven by a combined effect of protein coating and plasma modification. *Biofabrication*, *2*(1).

Zhang, J., Qi, H. X., Wang, H. J., Hu, P., Ou, L. L., Guo, S. H., et al. (2006). Engineering of vascular grafts with genetically modified bone marrow mesenchymal stem cells on poly (propylene carbonate) graft. *Artificial Organs*, *30*(12), 898–905.

Zhang, L., Zheng, Z. H., Xi, J., Gao, Y., Ao, Q., Gong, Y. D., et al. (2007). Improved mechanical property and biocompatibility of poly(3-hydroxybutyrate-co-3-hydroxyhexanoate) for blood vessel tissue engineering by blending with poly(propylene carbonate). *European Polymer Journal*, *43*(7), 2975–2986.

Zhao, J. H., Han, W. Q., Chen, H. D., Tu, M., Huan, S. W., Miao, G. Q., et al. (2012). Fabrication and in vivo osteogenesis of biomimetic poly(propylene carbonate) scaffold with nanofibrous chitosan network in macropores for bone tissue engineering. *Journal of Materials Science-Materials in Medicine*, *23*(2), 517–525.

Zhao, J. H., Han, W. Q., Tu, M., Huan, S. W., Zeng, R., Wu, H., et al. (2012). Preparation and properties of biomimetic porous nanofibrous poly(l-lactide) scaffold with chitosan nanofiber network by a dual thermally induced phase separation technique. *Materials Science and Engineering C—Materials for Biological Applications*, *32*(6), 1496–1502.

Zhu, A. P., Zhao, F., & Ma, T. (2009). Photo-initiated grafting of gelatin/N-maleic acyl-chitosan to enhance endothelial cell adhesion, proliferation and function on PLA surface. *Acta Biomaterialia*, *5*(6), 2033–2044.

Zhu, Y. B., Gao, C. Y., He, T., Liu, X. Y., & Shen, J. C. (2003). Layer-by-layer assembly to modify poly(L-lactic acid) surface toward improving its cytocompatibility to human endothelial cells. *Biomacromolecules*, *4*(2), 446–452.